Intracellular calcium movements during excitation–contraction coupling in mammalian slow-twitch and fast-twitch muscle fibers

Stephen M. Baylor and Stephen Hollingworth

Department of Physiology, University of Pennsylvania, Philadelphia, PA 19104

In skeletal muscle fibers, action potentials elicit contractions by releasing calcium ions (Ca^{2+}) from the sarcoplasmic reticulum. Experiments on individual mouse muscle fibers micro-injected with a rapidly responding fluorescent Ca^{2+} indicator dye reveal that the amount of Ca^{2+} released is three- to fourfold larger in fast-twitch fibers than in slow-twitch fibers, and the proportion of the released Ca^{2+} that binds to troponin to activate contraction is substantially smaller.

INTRODUCTION

The skeletal muscles of mammals account for ∼40% of body weight and for ∼25% of the basal metabolic rate (Rolfe and Brown, 1997). Approximately half of this muscle mass consists of slow-twitch fibers, and the other half consists of fast-twitch fibers (also called type I and type II fibers, respectively). Small numbers of other fiber types, such as superfast fibers and true-slow fibers, are also found in specialized muscles such as eye and jaw muscles (Hess, 1970; Hoh, 2002; Andrade et al., 2005). The basic unit of activity in the two main fiber types is the "twitch," in which a single action potential (AP) on the fiber's surface membrane elicits a brief contractile response. This article concerns the transient increase in the myoplasmic free calcium concentration ($\Delta[Ca^{2+}]$), which is the key intermediate signaling event between excitation and contraction. As $[Ca^{2+}]$ rises, Ca^{2+} binds to troponin, a regulatory protein on the actin filament, thereby enabling myosin to interact with actin and generate the contractile response. When $[Ca^{2+}]$ falls, Ca^{2+} dissociates from troponin and contractile activity declines.

Slow-twitch fibers have many similarities and also some important differences when compared with fast-twitch fibers (Berchtold et al., 2000; Allen et al., 2008; Schiaffino and Reggiani, 2011). Slow-twitch fibers are more resistant to fatigue than fast-twitch fibers, partly because of their larger mitochondrial volume and higher activity of oxidative enzymes (Schwerzmann et al., 1989; Jackman and Willis, 1996). Also, as the naming system implies, the time course of the contractile response of slow-twitch fibers is substantially slower than that of fast-twitch fibers. For example, in rat motor units studied in the anesthetized animal, the time of peak of the twitch response and the time between peak and half-relaxation are three- to fivefold larger in slow-twitch units of the soleus muscle than in fast-twitch units of the extensor digitorum longus (EDL) muscle (Table 1, A). Similar differences in twitch kinetics are found in individual fibers and in small bundles of fibers from mouse soleus and EDL muscles studied after removal of the muscles from the animal (Table 1, B and C).

Part of the difference in contractile speed between slow-twitch and fast-twitch fibers is attributable to a difference in myosin isoforms. For example, in rat muscle, the major myosin isoform found in soleus fibers has a cycling rate at saturating $[Ca^{2+}]$ that is about one third of that of the major isoform in EDL fibers (Unsworth et al., 1982; Bottinelli et al., 1994). Some of the fiber-type differences in twitch kinetics likely also arise because of differences in $\Delta[Ca^{2+}]$ (see below) and in the troponin isoforms (van Eerd and Takahashi, 1976; Potter et al., 1977; Sweeney et al., 1990).

The Ca^{2+} cycle during a muscle twitch

Fig. 1 diagrams the major intracellular movements of Ca^{2+} that take place during a twitch. An AP initiated on the surface membrane propagates into the transverse (T)-tubular system, where specialized voltage-sensing molecules (dihydropyridine receptors [DHPRs]) move to their activating position (Schneider and Chandler, 1973; Hollingworth and Marshall, 1981; Ríos and Brum, 1987; Tanabe et al., 1988). The DHPRs then activate the SR Ca^{2+} release channels, whose large cytoplasmic domain spans the gap between the T-tubular and SR membranes at the triadic junction (Franzini-Armstrong and Nunzi, 1983). As the release channels open, Ca^{2+} moves from the SR into the myoplasm under a large chemical driving force. A large local increase in $[Ca^{2+}]$ ensues, which drives the diffusion of Ca^{2+} throughout the sarcomere (Cannell and Allen, 1984; Escobar et al., 1994; Baylor

Correspondence to Stephen M. Baylor: baylor@mail.med.upenn.edu

Abbreviations used in this paper: AP, action potential; DHPR, dihydropyridine receptor; EDL, extensor digitorum longus; FDHM, full duration at half-maximum.

The Rockefeller University Press
J. Gen. Physiol. Vol. 139 No. 4 261–272
www.jgp.org/cgi/doi/10.1085/jgp.201210773

TABLE 1

Twitch kinetics of motor units and muscle fibers from young adult rats and mice

Experimental preparation	*n*	Time of peak	Half-relaxation time	FDHM
		ms	*ms*	*ms*
A. Motor units in anesthetized rats[a] (normal sarcomere length; 35-36°C)				
1. Soleus muscle (slow-twitch units)	34	38 ± 4	57 ± 8	—
2. EDL muscle (fast-twitch units)	48	11 ± 1	11 ± 2	—
B. Singly dissected mouse fibers[b] (normal sarcomere length; 20-21°C)				
1. Soleus fibers (slow-twitch)	12	96 ± 7.5	130 ± 14	—
2. EDL fibers (fast-twitch)	11	33 ± 6.1	62 ± 12	—
C. Small bundles of mouse fibers[c] (long sarcomere length; 16°C)				
1. Soleus fibers (slow-twitch)	14	173 ± 9	708 ± 73	843 ± 80
2. EDL fibers (fast-twitch)	16	52 ± 2	162 ± 11	197 ± 12

n is the number of motor units (A) or experiments (B and C). Time of peak is the time between the external stimulus and the peak of the twitch tension response, half-relaxation time is the time between the peak and half-decay of tension, and FDHM is the time between the half-rise and half-decay of tension. In A and B, the sarcomere length was set to give the maximum tension response. In C, average sarcomere length was 3.7 µm (range, 3.3–3.9 µm).
[a]Close, 1967.
[b]González et al., 2000.
[c]Hollingworth et al., 1996, 2008, 2012; and Baylor and Hollingworth, 2003.

and Hollingworth, 1998; Hollingworth et al., 2000; Gómez et al., 2006). As Ca^{2+} diffuses, it binds to sites on various myoplasmic constituents (termed Ca^{2+} "buffers" in this article), the most important of which are indicated in Fig. 1: (a) troponin, which, as noted above, has regulatory sites (Ca^{2+}-specific sites) that mediate contractile activation; (b) ATP, which acts as a mobile buffer for Ca^{2+} and Mg^{2+}; (c) more slowly reacting, less mobile buffers for Ca^{2+} and Mg^{2+} ("SlowB"), such as parvalbumin; and (d) the SR Ca^{2+} pump, which resequesters Ca^{2+} within the SR, translocating two Ca^{2+} ions for each ATP consumed (Weber et al., 1966). (e) If a Ca^{2+} indicator dye is introduced into the myoplasm, some Ca^{2+} will also bind to the dye. If the indicator is well chosen and other features of the experiment are favorably arranged, the optical signal from the indicator can be used to monitor the amplitude and time course of $\Delta[Ca^{2+}]$ (described in next section). From $\Delta[Ca^{2+}]$ and information from the literature about the concentrations and kinetic reactions of the major myoplasmic Ca^{2+} buffers, quantitative

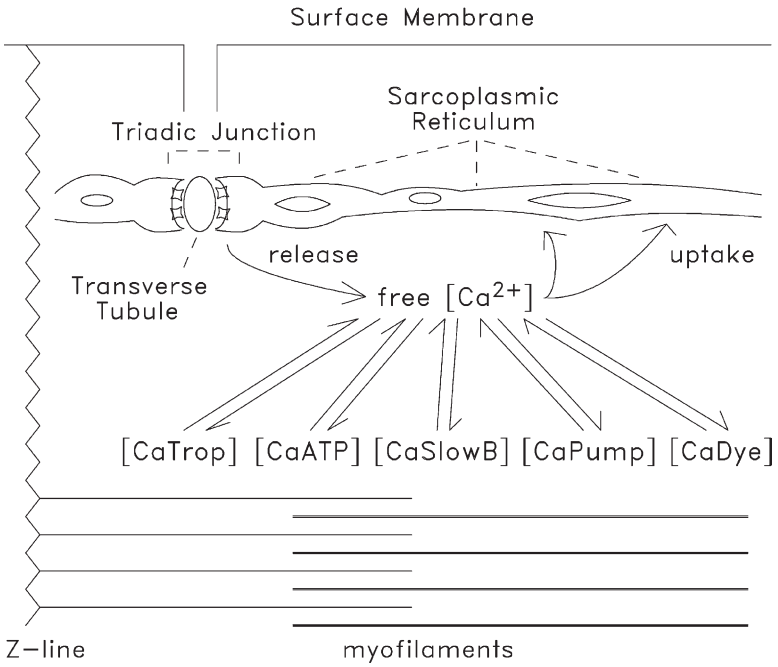

Figure 1. Schematic of intra-sarcomeric Ca^{2+} movements during excitation–contraction coupling in mammalian skeletal muscle fibers. Depolarization of the transverse tubular membranes initiates Ca^{2+} release from the SR at the triadic junctions. The rise in myoplasmic free $[Ca^{2+}]$ drives Ca^{2+} complexation with the major myoplasmic Ca^{2+} buffers: (a) troponin (located on the thin filaments); (b) ATP; (c) other proteins ("SlowB") such as parvalbumin, which, in rodent fibers, is found at a large concentration in fast-twitch glycolytic fibers but not in slow-twitch fibers (Table 2); (d) Ca^{2+} pump molecules (located in the SR membranes); and (e) the Ca^{2+} indicator dye (which can be introduced experimentally to monitor $\Delta[Ca^{2+}]$).

estimates can be made about the complexation of Ca^{2+} with the buffers and thus about the amount and time course of SR Ca^{2+} release and reuptake (compare calculations described below).

Comparison of $\Delta[Ca^{2+}]$ in slow-twitch and fast-twitch mouse fibers

Several different Ca^{2+} indicators have been used in skeletal muscle fibers in pursuit of a reliable method to measure the amplitude and time course of $\Delta[Ca^{2+}]$ (Baylor and Hollingworth, 2011). Furaptra (also called mag-fura-2; Raju et al., 1989), which is a fluorescent Ca^{2+} indicator of the "tricarboxylate" family, has yielded some of the most useful quantitative information to date about $\Delta[Ca^{2+}]$ (Konishi et al., 1991; Delbono and Stefani, 1993; Claflin et al., 1994; Delbono and Meissner, 1996; Hollingworth et al., 1996, 2008, 2012; Rome et al., 1996; Baylor and Hollingworth, 2003, 2007; Harwood et al., 2011). Furaptra's chromophore, which is similar to that of fura-2 (Grynkiewicz et al., 1985), undergoes a large change in both absorbance and fluorescence upon binding Ca^{2+}. In contrast with fura-2, furaptra has a low affinity for Ca^{2+}, with a dissociation constant ($K_{D,Ca}$) that is estimated to be 96 µM in the myoplasmic environment (Konishi et al., 1991; Baylor and Hollingworth, 2003). Because furaptra's low affinity is achieved by virtue of a fast off-rate constant for Ca^{2+}, which is probably at least several thousand per second in myoplasm at 20°C (Naraghi, 1997; Baylor and Hollingworth, 1998), furaptra should always respond rapidly to changes in $[Ca^{2+}]$. These features make furaptra a very valuable indicator for measuring the large and brief $\Delta[Ca^{2+}]$ that occurs in skeletal muscle fibers during AP-evoked activity. Some valuable kinetic information about $\Delta[Ca^{2+}]$ in mammalian fibers has also been obtained with mag-fluo-4 (Capote et al., 2005; Calderón et al., 2009, 2010; Hollingworth et al., 2012), another low-affinity tricarboxylate fluorescent indicator that reacts rapidly with Ca^{2+} (Hollingworth et al., 2009).

Fig. 2 A shows examples of indicator-related Ca^{2+} signals (top two rows of traces) and tension responses (third row of traces) recorded in mouse soleus fibers that were activated by a single AP (dashed traces) or a brief high-frequency train of APs (five APs at 67 Hz; continuous traces). Fig. 2 B shows similar recordings in EDL fibers. The traces are averaged results from several similar experiments in which one fiber within a bundle of intact fibers was micro-injected with the membrane-impermeant (K^+ salt) form of either furaptra or mag-fluo-4; thus, only one fiber contributed to the change in fluorescence (ΔF) in each experiment. Based on the markedly different speeds of the contractile responses in Fig. 2 (see legend), the fibers from soleus and EDL muscles have been classified as slow-twitch and fast-twitch, respectively; biochemical properties such as the myosin heavy chain isoform were not determined.

In the recordings in Fig. 2, the indicator's fluorescence was collected from a length of fiber of ∼300 µm; thus, the fluorescence signals represent a spatial average from many sarcomeres. To ensure that the fluorescence signals were minimally influenced by movement artifacts, the fibers were stretched to a long sarcomere length (average value of 3.7 µm), which greatly reduces the fiber's contractile response. The raw indicator measurements (topmost traces in Fig. 2) are shown in units of furaptra's $\Delta F/F_R$, the change in the indicator's fluorescence divided by its resting fluorescence. The second row of traces shows the $\Delta F/F_R$ waveforms transformed to units of $\Delta[Ca^{2+}]$ based on a two-step procedure (Baylor and Hollingworth, 2003). In the first step, the $\Delta F/F_R$ traces were scaled by the factor −1.07 (a calibration constant specific to furaptra fluorescence measured with excitation wavelengths of 410 ± 20 nm and emission wavelengths of 530 ± 60 nm), which converts the fluorescence change to the underlying change in the fraction of furaptra bound with Ca^{2+}, Δf_{CaD}. The Δf_{CaD} traces are shown in Fig. 2 (C and D; traces with noise, which are described further below). In the second step, the Δf_{CaD} traces were converted to $\Delta[Ca^{2+}]$ with the equation for 1:1 binding between Ca^{2+} and a low-affinity indicator: $\Delta[Ca^{2+}] = K_{D,Ca} \cdot \Delta f_{CaD}/(1 - \Delta f_{CaD})$. As described in the next section, a more accurate estimate of spatially averaged $\Delta[Ca^{2+}]$ can be obtained from the Δf_{CaD} traces with a different analytical approach.

In Fig. 2 A, $\Delta[Ca^{2+}]$ during a single twitch in slow-twitch fibers has a peak of ∼10 µM and a full duration at half-maximum (FDHM) of ∼8 ms; the corresponding values in fast-twitch fibers are ∼18 µM and ∼5 ms, respectively (Fig. 2 B). These differences between fiber types are highly reproducible and are diagnostic of the fiber type (Hollingworth et al., 2012). During the high-frequency stimulation (five APs at 67 Hz), peak $\Delta[Ca^{2+}]$ in slow-twitch fibers rises ∼20% above that elicited by the first AP; in contrast, in fast-twitch fibers, the peaks of $\Delta[Ca^{2+}]$ elicited by subsequent APs have about the same amplitude as that elicited by the first AP. In both fiber types, the rate of decay of $\Delta[Ca^{2+}]$ from its fifth peak is much smaller than that from its first peak. As described below, the reason for the progressive decrease in this decay rate with later APs in the train is that there is a progressive increase in the occupancy of the myoplasmic Ca^{2+} buffers with Ca^{2+} and, consequently, a decrease in the rate at which the buffers bind Ca^{2+} (Melzer et al., 1987; Hollingworth et al., 1996, 2012; Carroll et al., 1997; Baylor and Hollingworth, 2007).

Simulation of myoplasmic Ca^{2+} movements with a reaction–diffusion model

Given the spatially averaged estimate of $\Delta[Ca^{2+}]$ obtained from the furaptra Δf_{CaD} signal (Fig. 2), a spatially averaged estimate of the change in concentration of Ca^{2+} bound to the sites on any particular myoplasmic Ca^{2+} buffer can

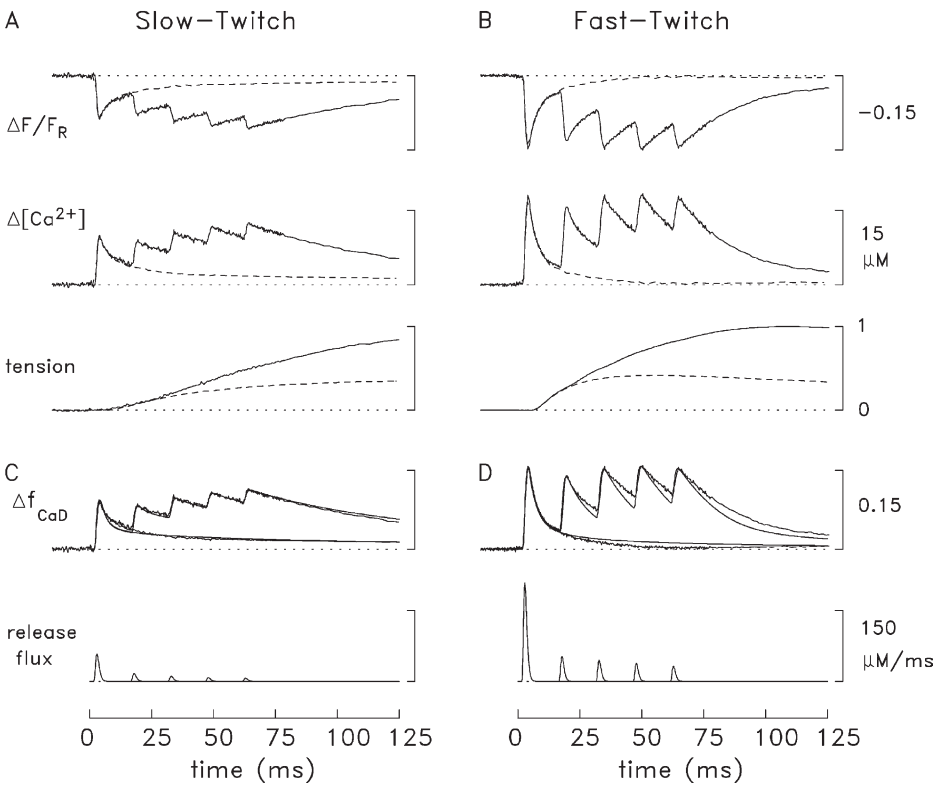

Figure 2. Ca^{2+}-related fluorescence signals and tension responses in slow-twitch and fast-twitch mouse fibers stimulated by APs (16°C). (A and B) Bundles of fibers from soleus muscles (A) and EDL muscles (B) of adult mice, age 7–14 wk, were isolated by dissection, and one fiber within the bundle was micro-injected with either furaptra or mag-fluo-4. $\Delta F/F_R$ and tension responses were recorded in response to external stimuli that elicited either one AP (dashed traces) or five APs at 67 Hz (continuous traces); the responses to both types of stimulation are shown superimposed. All traces represent averaged responses from several experiments in which movement artifacts in the $\Delta F/F_R$ traces were small. All fast-twitch experiments were performed on fibers injected with furaptra (seven fibers in the measurements with a single AP, four in the measurements with five APs); the fast-twitch fibers are from a region of the EDL muscle thought to be rich in parvalbumin (see Baylor and Hollingworth, 2011). The slow-twitch experiments with a single AP are from 11 experiments (five with furaptra and six with mag-fluo-4); those with five APs are from three experiments (one with furaptra and two with mag-fluo-4). Before inclusion in the average responses, the mag-fluo-4 traces were scaled so that their amplitude matched that expected with furaptra (Hollingworth et al., 2009, 2012). $\Delta F/F_R$, in furaptra fluorescence units, was converted to Δf_{CaD} and $\Delta[Ca^{2+}]$ as described in the text. For both fiber types, a value of 1 on the tension calibration bar corresponds to the peak tension response with the five-AP stimulus. With one AP, the time of peak and FDHM of the slow-twitch tension response are 192 and 1,001 ms, respectively; the corresponding values for the fast-twitch tension response are 55 and 215 ms; with the five-AP stimulus, the values are 229 and 993 ms for the slow-twitch response and 107 and 236 ms for the fast-twitch response. (C and D) The top traces show simulated furaptra Δf_{CaD} waveforms (noise-free traces) and measured Δf_{CaD} waveforms (traces with noise). The simulated traces were obtained with the multi-compartment model described in Fig. 3 and the text. In the model, the reaction scheme between Ca^{2+} and furaptra includes two pools of furaptra, protein-free and protein-bound (Baylor and Hollingworth, 2007); the protein-bound pool corresponds to the indicator molecules that appear to be bound to myoplasmic constituents of low mobility (Konishi et al., 1991). The bottom traces show the SR Ca^{2+} fluxes used to drive the simulations. Even though the measurements were made with the fibers stretched to a long sarcomere length (mean value, 3.7 μm), the experimental Δf_{CaD} traces may still be slightly contaminated with a small movement artifact.

be calculated if the buffer concentration is known and a reaction scheme and reaction rate constants are available for the site (e.g., Robertson et al., 1981; Baylor et al., 1983; Cannell and Allen, 1984; Hollingworth et al., 2006; see also Fig. 5, described below). Table 2 lists the concentrations of the buffer sites considered in the calculations described here and in the next section; the reaction schemes and rate constants are given in Baylor and Hollingworth (2007) and Hollingworth et al. (2012). If the calculated changes in concentration of Ca^{2+} bound to these various buffers are summed and added to that of $\Delta[Ca^{2+}]$ plus Δ[CaDye], one obtains a spatially averaged estimate of the total concentration of Ca^{2+} released by the SR. A more accurate estimate of $\Delta[Ca^{2+}]$ and the other Ca^{2+} changes, however, can be obtained if the Δf_{CaD} signal from the indicator is simulated with a multi-compartment model of the myoplasmic Ca^{2+} movements based on a reaction–diffusion model (Cannell and Allen, 1984; Baylor and Hollingworth, 1998, 2007; Jiang et al., 1999; Novo et al., 2003; Hollingworth et al., 2012). Models of this type, in addition to using information about the reactions of Ca^{2+} with its buffers, incorporate information about (a) the dimensions of the sarcomere; (b) the locations of the Ca^{2+} release sites, the Ca^{2+} buffers, and Ca^{2+} pumping; and (c) the myoplasmic diffusion coefficients of the mobile myoplasmic constituents (free Ca^{2+}, mobile buffers such as ATP, etc.). Calculations with these models reveal steep gradients in $\Delta[Ca^{2+}]$ within the sarcomere. One consequence of these gradients is that the degree of saturation of the buffers with Ca^{2+} varies markedly at different times and sarcomeric locations. In the case of furaptra, this variation introduces error into the estimation of $\Delta[Ca^{2+}]$ from the measured Δf_{CaD} signal and the 1:1 binding equation (Hirota et al., 1989; Baylor and Hollingworth, 1998, 2007). By taking into account the $\Delta[Ca^{2+}]$ gradients, reaction–diffusion models are thought

to yield more accurate estimates of spatially averaged $\Delta[Ca^{2+}]$, of the amplitude and time course with which Ca^{2+} binds to the myoplasmic Ca^{2+} buffers, and of the amount of SR Ca^{2+} release.

Fig. 3 diagrams the multi-compartment model that we have used in the analysis of the furaptra Ca^{2+} measurements in mouse fibers. The myoplasmic water volume of a half-sarcomere of one myofibril is considered to be the basic unit of interest, and this volume is divided into 18 compartments of equal size. The buffer concentrations, as well as the locations of SR Ca^{2+} release and pumping, are assigned appropriately to the various compartments (see legend of Fig. 3 and Table 2). To relate the calculations with the model to the furaptra measurements, the model is driven by an assumed waveform for the SR Ca^{2+} release flux. The time course of this flux is estimated from the single-compartment (spatially averaged) version of the model (Baylor et al., 1983; Hollingworth et al., 1996), for which the release flux is fully determined by $\Delta[Ca^{2+}]$ and the specified properties of the Ca^{2+} buffers. The amplitude of the flux waveform in the multi-compartment model is then adjusted iteratively until the amplitude of the simulated, spatially averaged Δf_{CaD} waveform matches that of the measured Δf_{CaD} waveform. The overall success of this approach is evaluated by a comparison of the time courses of the simulated and measured Δf_{CaD} waveforms. If these time courses are in agreement, it is reasonable to believe that the simulations give an approximate description of the underlying Ca^{2+} movements. In Fig. 2 (C and D), the top superimposed traces show examples of such comparisons, and the bottom traces show the SR Ca^{2+} release fluxes used to drive the simulations. The good agreement between the simulated Δf_{CaD} waveforms (noise-free traces) and the measured Δf_{CaD} waveforms (traces with noise) indicates that this strategy is successful in both fiber types.

TABLE 2

Concentrations of divalent ion–binding sites in the computational models

Type of site	Slow-twitch fibers	Fast-twitch fibers
	μM	*μM*
Ca^{2+}-specific sites:		
Troponin regulatory sites[a]	120	240
Ca^{2+}/Mg^{2+} sites:		
ATP[b] (one per molecule)	5,000	8,000
SlowB (slow-buffer sites)		
Parvalbumin[c] (two/molecule)	0	1,500
Troponin-nonspecific sites[d] (two/molecule)	240	0
Ca^{2+} pump[e] (two per molecule)	96	240
Furaptra[f] (one per molecule)	100	100

The site concentrations are spatially averaged and referred to the myoplasmic water volume (Baylor et al., 1983). The fast-twitch model ignores the 240-μM troponin-nonspecific sites (Ca^{2+}/Mg^{2+} sites) because their buffering effect is small compared with the sites on parvalbumin, which are present in the fast-twitch model at a large concentration. Other myoplasmic Ca^{2+}-binding sites, such as those on inorganic phosphate, calmodulin, calpain, calcineurin, sorcin, annexin, S100A, the plasmalemma Ca^{2+} pump, and the Na^{+}/Ca^{2+} exchanger, have been ignored because their concentrations are small relative to those of the major buffers listed in the table. The kinetic parameters for the sites at 16°C are given in Baylor and Hollingworth (2007) and Hollingworth et al. (2012). Both models assume that free $[Ca^{2+}]$ at rest is 0.05 μM and that free $[Mg^{2+}]$ is 1 mM and constant.

[a]van Eerd and Takahashi, 1976; Potter et al., 1977; and Robertson et al., 1981.

[b]Kushmerick et al., 1992, and Racay et al., 2006.

[c]Heizmann et al., 1982, and Leberer and Pette, 1986.

[d]Robertson et al., 1981.

[e]Ferguson and Franzini-Armstrong, 1988.

[f]Baylor and Hollingworth, 2007, and Hollingworth et al., 2012.

Comparison of myoplasmic Ca^{2+} movements in slow-twitch and fast-twitch fibers

Fig. 4 summarizes some results from these multi-compartment simulations. Responses in slow-twitch and fast-twitch fibers are shown as continuous and dashed traces, respectively. Fig. 4 A compares responses to a single

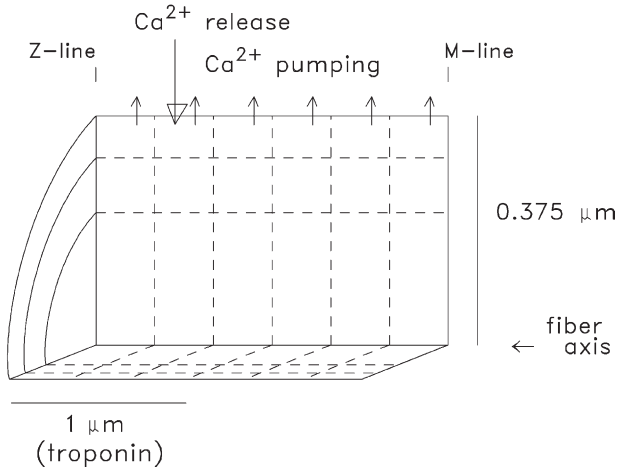

Figure 3. Geometry of the multi-compartment reaction–diffusion model used to simulate myoplasmic Ca^{2+} movements. The myoplasm of a half-sarcomere of one myofibril is divided into 18 equal-volume radially symmetric compartments (six longitudinal by three radial) at a half-sarcomere length of 2 μm. Ca^{2+} release (large downward arrow) occurs into the compartment located at the periphery of the myofibril about ∼0.5 μm from the z-line, the location of the triadic junctions in mammalian fibers (Smith, 1966; Eisenberg, 1983; Brown et al., 1998; Gómez et al., 2006). Ca^{2+} pumping (small upward arrows) is restricted to the six outermost compartments at the periphery of the myofibril (the location of the SR membrane), troponin is restricted to the nine compartments located within 1 μm of the z-line (the location of the thin filaments), and free Ca^{2+} and the soluble Ca^{2+} buffers (e.g., ATP, parvalbumin, and the Ca^{2+} indicator) have access to all compartments via diffusion. The buffer concentrations and reaction rate constants vary with the fiber type and compartment location (see text and Table 2). A set of first-order differential equations is specified for each compartment to describe the Ca^{2+} concentration changes that take place in that compartment caused by release, binding, pumping, and/or diffusion across compartment boundaries. The full set of equations can be integrated simultaneously once the SR Ca^{2+} release flux is specified.

AP, and B compares them to five APs at 67 Hz. For simplicity in the presentation, all waveforms in Fig. 4 have been spatially averaged; i.e., each trace was calculated as the average of the corresponding changes in the 18 compartments of the model. (Examples of waveforms calculated for the individual compartments are given in Baylor and Hollingworth, 2007). The traces in Fig. 4 are (from bottom to top): (a) $\Delta[Ca^{2+}]$; (b) the change in concentration of Ca^{2+} bound to the regulatory sites on troponin (Δ[CaTrop]); (c) the fractional occupancy of the troponin regulatory sites with Ca^{2+} (f_{CaTrop}, which, for this variable, includes the resting occupancy); (d) the change in concentration of Ca^{2+} bound to the sites on the slowly reacting buffers (Δ[CaSlowB], which includes Ca^{2+} binding to parvalbumin in fast-twitch fibers and to the troponin-nonspecific sites in slow-twitch fibers; see Table 2); (e) the change in concentration of Ca^{2+} bound to the SR Ca^{2+} pumps (Δ[CaPump]); (f) the change in concentration of Ca^{2+} returned to the SR as a result of Ca^{2+} pumping (Δ[CaPumped]); and (g) the total concentration of released Ca^{2+} ($\Delta[Ca_T]$). Not shown, but included in the calculation of $\Delta[Ca_T]$, are Δ[CaATP] and Δ[CaDye] (see legend of Fig. 4). Except for f_{CaTrop}, these traces are shown in concentration units referred to the myoplasmic water volume.

In Fig. 4 A, peak $\Delta[Ca_T]$ in response to one AP in a slow-twitch fiber is 107 μM, which is achieved with a peak SR Ca^{2+} flux of 57 μM/ms and a flux FDHM of 1.7 ms (see also Fig. 2 C); the corresponding values for a fast-twitch fiber are 349 μM, 205 μM/ms, and 1.6 ms (see also Fig. 2 D). The modeled spatially averaged $\Delta[Ca^{2+}]$ in slow-twitch fibers has a peak amplitude of 7.6 μM and an FDHM of 4.9 ms. As expected from Fig. 2, the corresponding values in fast-twitch fibers are larger and briefer, 16.1 μM and 3.7 ms. These properties of spatially averaged $\Delta[Ca^{2+}]$ obtained with the multi-compartment models are thought to be more accurate than those obtained above with the single-compartment analysis (Fig. 2, A and B). The multi-compartment estimates of the FDHM of $\Delta[Ca^{2+}]$ are substantially briefer: 4.9 versus 8 ms for slow-twitch fibers and 3.7 versus 5 ms for fast-twitch fibers. In both fiber types, peak $\Delta[Ca^{2+}]$ is a small fraction of peak $\Delta[Ca_T]$ (<0.1); i.e., the great majority of the released Ca^{2+} is rapidly bound by the Ca^{2+} buffers, with only a small fraction remaining free.

In Fig. 4 A, peak Δ[CaTrop] shows a large difference between the two fiber types: 86 μM for slow-twitch fibers and 227 μM for fast-twitch fibers. This difference arises primarily because fast-twitch troponin has two Ca^{2+} regulatory sites per molecule, whereas slow-twitch troponin has only one (van Eerd and Takahashi, 1976; Potter et al., 1977; Robertson et al., 1981; Sweeney et al., 1990). If, however, the concentration of Ca^{2+} bound to the troponin regulatory sites is normalized by the total concentration of these sites (120 μM in slow-twitch fibers and 240 μM in fast-twitch fibers; Table 2), peak f_{CaTrop} is similar in slow-twitch and fast-twitch fibers: 0.79 and 0.95, respectively. Δ[CaSlowB] is also very different in the two fiber types, with values of 9 and 146 μM, respectively, at t = 50 ms. This difference reflects the large concentration

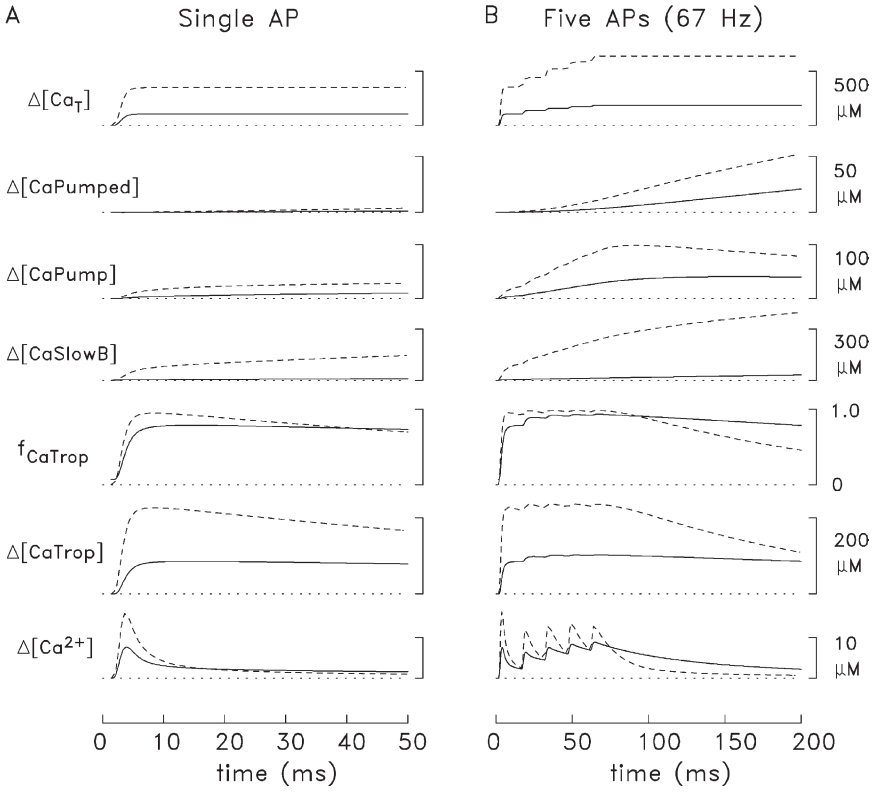

Figure 4. Comparison of Ca^{2+} movements elicited by APs in slow-twitch and fast-twitch fibers (16°C). (A). Simulated Ca^{2+} movements in slow-twitch and fast-twitch fibers (continuous and dashed traces, respectively) in response to a single AP initiated at zero time. f_{CaTrop}, the fractional occupancy of the troponin regulatory sites with Ca^{2+}, includes the resting occupancy (0.071 in slow-twitch fibers and 0.004 in fast-twitch fibers) plus the change in occupancy during activity. See text for definitions of the other traces. $\Delta[Ca_T]$ is the sum of the five lower traces, excluding f_{CaTrop}, plus Δ[CaATP] and Δ[CaDye] (the change in the concentration of Ca^{2+} bound to the indicator). Δ[CaATP] is approximately equal to 2.2 times $\Delta[Ca^{2+}]$ in slow-twitch fibers and 3.4 times $\Delta[Ca^{2+}]$ in fast-twitch fibers. Δ[CaDye] is relatively small (= $\Delta f_{CaD} \times [Dye_T]$, where $[Dye_T]$, the total indicator concentration in myoplasm, is 100 μM). The units of all traces except f_{CaTrop} are spatially averaged concentrations referred to the myoplasmic water volume. (B). As in A, but for five APs at 67 Hz.

of parvalbumin that is found in mouse fast-twitch glycolytic fibers compared with slow-twitch fibers, which have little or no parvalbumin (compare Table 2). Δ[CaPump] is also quite different in the two fiber types, with 10 µM in slow-twitch fibers and 28 µM in fast-twitch fibers at t = 50 ms. The primary reason is that the concentration of Ca^{2+} pump molecules is larger in fast-twitch fibers: 120 versus 48 µM (Table 2). A second reason is that, because $\Delta[Ca^{2+}]$ is larger in fast-twitch fibers, the fractional occupancy of the pump sites with Ca^{2+} is larger. (Note: fast-twitch and slow-twitch fibers have different proportions of the two main isoforms of the Ca^{2+} pump molecules found in skeletal muscle, denoted SERCA1 and SERCA2a, but the functional properties of the two isoforms are similar; Lytton et al., 1992; Wu and Lytton, 1993.) Because of the larger amplitude of Δ[CaPump] in fast-twitch fibers, Δ[CaPumped] is also larger, with values at t = 50 ms of 3.7 µM for fast-twitch fibers and 1.1 µM for slow-twitch fibers. Ca^{2+} pumping is a relatively slow process, with an estimated turnover rate at saturating $[Ca^{2+}]$ of 3–4 s^{-1} (16°C; Inesi et al., 1982; Young et al., 2003); thus, the resequestration of the released Ca^{2+} into the SR is not expected to be completed until several seconds after stimulation.

Fig. 4 B, which compares responses for the case of five APs at 67 Hz, reveals several new features. First, in both fiber types, the increments in $\Delta[Ca_T]$ caused by the second through fifth APs are much smaller than that caused by the first. Considered as a fraction of the first release, the values vary from 0.30 to 0.13 in slow-twitch fibers and from 0.26 to 0.15 in fast-twitch fibers (see also bottommost traces in Fig. 2). These marked reductions in release are thought to be caused primarily by the process of Ca^{2+} inactivation of Ca^{2+} release, in which a rise in $[Ca^{2+}]$ is sensed by the release system to inhibit release (Baylor et al., 1983; Schneider and Simon, 1988; Baylor and Hollingworth, 1988, 2007; Jong et al., 1995). The molecule(s) that mediates this negative feedback remains to be fully identified, although an interaction between calmodulin and an identified site on the SR release channel may be involved (Yamaguchi et al., 2011). This feedback has an obvious physiological function, as it prevents $[Ca^{2+}]$ from rising to higher levels than is required to activate the myofilaments, thereby avoiding: (a) an unnecessary delay in fiber relaxation after cessation of APs, (b) extra expenditure of ATP by the Ca^{2+} pumps to resequester Ca^{2+}, and (c) potential damage to the mitochondria caused by excessive uptake of Ca^{2+}.

A second noteworthy feature in Fig. 4 B is that peak f_{CaTrop} is close to 1 in both fiber types: 0.93 in slow-twitch fibers and 0.96 in fast-twitch fibers. Thus, in both fiber types, the models predict that $\Delta[Ca^{2+}]$ during repetitive stimulation rises to a level at which activation of the myofilaments is not limited by $[Ca^{2+}]$. The conclusion that the troponin regulatory sites are rapidly and nearly completely occupied with Ca^{2+} in both fiber types while the rate of tension development is much slower in slow-twitch than in fast-twitch fibers (see tension traces in Fig. 2, A and B) is consistent with observations in chemically skinned rodent fibers that the rate at which myosin produces force at saturating $[Ca^{2+}]$ is inherently slower with slow-twitch than with fast-twitch myosin (Metzger and Moss, 1990). Because the troponin regulatory sites and the sites on the other buffers (e.g., "SlowB") become increasingly occupied with Ca^{2+} during the high-frequency stimulus, the ability of these sites to bind newly released Ca^{2+} decreases; as a result, there is a progressive decrease in the rate of decay of $\Delta[Ca^{2+}]$ from its individual peaks during the train. Consistent with the longer lasting $\Delta[Ca^{2+}]$ waveform, Δ[CaSlowB], Δ[CaPump], and Δ[CaPumped] all rise to substantially higher levels than those that occur with a single AP.

Functional differences between Ca^{2+} movements in slow-twitch and fast-twitch fibers

As noted above, the calculations indicate that the troponin regulatory sites rapidly bind a large fraction of the released Ca^{2+} in both slow-twitch and fast-twitch fibers. The fraction is smaller in fast-twitch fibers, however, because fast-twitch fibers have relatively larger concentrations of sites on the other buffers (Table 2), which compete with troponin for Ca^{2+}. Thus, to achieve full occupancy of their regulatory sites, fast-twitch fibers must release substantially more Ca^{2+} than is expected from their twofold larger concentration of regulatory sites. The ability of fast-twitch fibers to release three- to fourfold larger amounts of Ca^{2+} than slow-twitch fibers (topmost traces in Fig. 4) at three- to fourfold larger rates (bottommost traces in Fig. 2) is achieved by means of comparable increases in the fractional volume of their SR (Eisenberg, 1983) and, concomitantly, in the number of the SR Ca^{2+} release channels and their controlling DHPR molecules (Hollingworth and Marshall, 1981; Lamb and Walsh, 1987; Franzini-Armstrong et al., 1988; Delbono and Meissner, 1996). The functional advantage of the large concentration of the slow-buffer sites in fast-twitch fibers is that a substantial fraction of the Ca^{2+} that is initially bound by troponin is subsequently bound by these sites (Gillis et al., 1982; Baylor et al., 1983; see also Fig. 4). By serving as a temporary myoplasmic storage site for released Ca^{2+}, the slow buffers contribute importantly to the more rapid decline of $\Delta[Ca^{2+}]$ that occurs in fast-twitch fibers, which helps to speed their contractile relaxation. An example of this slow-buffer function taken to an extreme occurs in the superfast swimbladder fibers of the toadfish (*Opsanau tau*), where the concentration of parvalbumin is nearly fourfold larger than that in mouse fast-twitch fibers (2.7 vs. 0.75 mM; Hamoir et al., 1980; Appelt et al., 1991; Tikunov and Rome, 2009), and the unusually brief $\Delta[Ca^{2+}]$ elicited by an AP in swimbladder fibers can be maintained for extended periods at stimulation frequencies

as high as 100 Hz (16°C; Rome et al., 1996; Harwood et al., 2011).

Fig. 5 illustrates several relevant differences between the modeled troponin reactions in slow-twitch and fast-twitch fibers. Ca^{2+} binds to the single regulatory site on each slow-twitch troponin molecule with a simple 1:1 reaction (Fig. 5 A), whereas Ca^{2+} binds to the two sites on each fast-twitch troponin molecule in a two-step reaction (Fig. 5 B). The rate constants for the slow-twitch reaction, which were estimated from information in Davis et al. (2007) in combination with comparisons of the type shown in Fig. 2 C (Hollingworth et al., 2012), are $0.4 \times 10^8\ M^{-1}\ s^{-1}$ for the on-rate (k_{+1}) and $26\ s^{-1}$ for the off-rate (k_{-1}) (16°C); the corresponding value of K_D ($= k_{-1}/k_{+1}$) is 0.65 µM. In contrast, with fast-twitch troponin, Ca^{2+} is thought to react with the two regulatory sites with positive cooperativity (Fuchs and Bayuk, 1976; Grabarek et al., 1983; see also Baylor et al., 2002). To achieve cooperativity in the modeled troponin reaction, the first Ca^{2+} ion binds with low affinity and the second with high affinity. The reaction rate constants are $k_{+1} = 1.77 \times 10^8\ M^{-1}\ s^{-1}$ and $k_{-1} = 1{,}542\ s^{-1}$ ($K_{D,1} = 8.72$ µM), and $k_{+2} = 0.885 \times 10^8\ M^{-1}\ s^{-1}$ and $k_{-2} = 17.1\ s^{-1}$ ($K_{D,2} = 0.193$ µM), respectively (Baylor et al., 2002; Davis, J.P., S.B. Tikunova, D.R. Swartz, and J.A. Rall. 2004. Biophysical Society 48th Annual Meeting. Abstr. 1135; Hollingworth et al., 2006). The steady-state level of free $[Ca^{2+}]$ that gives half-occupancy of these sites (Ca^{2+}_{50}) is 1.3 µM ($= \text{sqrt}(K_{D,1} \times K_{D,2})$), which is twice Ca^{2+}_{50} for the slow-twitch troponin reaction. These features are consistent with observations on mammalian skinned fibers that the tension–pCa curve in fast-twitch fibers is right-shifted with respect to that in slow-twitch fibers and has a steeper dependence on $[Ca^{2+}]$ (Kerrick et al., 1976; Stephenson and Williams, 1981; Ruff, 1989; Danieli-Betto et al., 1990). For example, in rat fibers, the $[Ca^{2+}]$ levels for half-activation of tension are ~1.2 and ~0.6 µM, respectively, for fast-twitch and slow-twitch fibers (22°C; sarcomere length of 2.7–2.8 µm; Stephenson and Williams, 1981).

Fig. 5 (C and D) presents a theoretical single-compartment analysis of some of the kinetic consequences of the modeled troponin reactions in the two fiber types. As revealed by this analysis, the more rapid rate of dissociation of Ca^{2+} from the regulatory sites that is observed in Fig. 4 B in fast-twitch fibers compared with slow-twitch fibers is explained by the more rapid decline of $\Delta[Ca^{2+}]$ in fast twitch fibers, not by an inherently faster rate of Ca^{2+} dissociation from the fast-twitch regulatory sites. In Fig. 5 C, the bottom trace shows a pulse of $[Ca^{2+}]$, which starts at 50 nM ($= [Ca^{2+}]_R$), rises in a square-wave fashion to 5 µM, where it remains for 50 ms, and then returns to the resting level, again in a square-wave fashion. The top trace shows the calculated Δ[CaTrop] response for slow-twitch troponin (compare Fig. 5 A), which rises exponentially from the resting level of 8.6 µM with a rate of $226\ s^{-1}$ to 106 µM (= 88.5% of saturation), and then decays back to the resting level with a rate of $28\ s^{-1}$. Fig. 5 D shows a similar calculation for the doubly occupied Ca^{2+} state of fast-twitch troponin (Ca_2Trop in Fig. 5 B), which is the troponin state that likely controls activation of the myofilaments. Here, the concentration of Ca^{2+} that is bound to the active state ($= 2 \times [Ca_2\text{Trop}]$) is 0.4 µM at rest and rises to 217 µM at peak (= 90.5% of saturation). Because the fast-twitch troponin reaction involves two-steps, neither the "on" nor "off" response exactly follows a single-exponential time course. Nevertheless, both responses are very well fitted by single-exponential time courses (not depicted), with effective on- and off-rates of 153 and $17.2\ s^{-1}$, respectively. The effective off-rate in Fig. 5 D is smaller than that in Fig. 5 C,

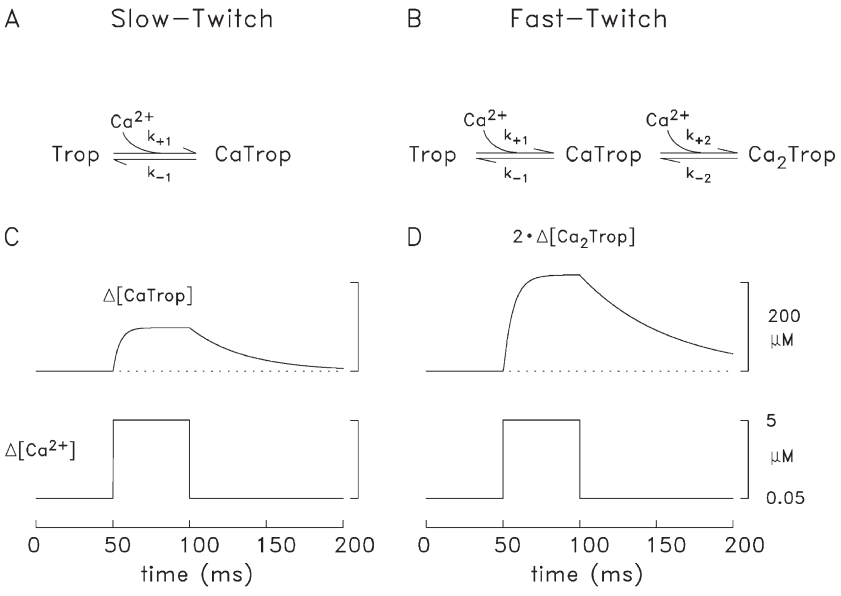

Figure 5. Comparison of the modeled Ca^{2+}–troponin reactions in slow-twitch and fast-twitch fibers. (A and B) Schemes for the reaction of Ca^{2+} with the regulatory sites on slow-twitch troponin (A) and fast-twitch troponin (B). The text gives the values of the reaction rate constants. (C and D) Theoretical single-compartment responses of the slow-twitch (C) and fast-twitch (D) troponin regulatory sites at 16°C to a pulse of $[Ca^{2+}]$ that starts at 50 nM, rises to 5 µM for 50 ms, and returns to 50 nM; the response in D considers only the doubly occupied troponin state in B. The total site concentrations are 120 µM (C) and 240 µM (D).

although Ca^{2+}_{50} is larger in fast-twitch than in slow-twitch fibers (1.3 vs. 0.65 µM). A significant advantage of the two-step cooperative troponin reaction (Fig. 5 B) is that it allows a more switchlike (all-or-nothing) control of the actomyosin system during activity. For example, the fraction of the troponin molecules in the activated state (the Ca_2Trop state) is negligible at rest in fast-twitch fibers (0.001), whereas, in slow-twitch fibers, the resting fraction in the CaTrop state (0.071) is not entirely negligible. The latter value would be expected to lead to a slight activation of the actomyosin system in slow-twitch fibers at rest and could contribute to the higher rate of resting energy consumption that has been reported in mouse soleus muscle compared with EDL muscle (Decrouy et al., 1993; Norris et al., 2010).

Calcium movements in slow-twitch and fast-twitch fibers at higher temperatures

The results described in connection with Figs. 2, 4, and 5 were obtained at 16°C, an experimental temperature that facilitates survival of the fibers outside the animal. To assess the functioning of the fibers at more physiological temperatures, some measurements like those in Fig. 2 have also been performed at higher temperatures (22, 28, and 35°C; Hollingworth et al., 1996, 2012; Baylor and Hollingworth, 2003). For example, in fibers at 28°C stimulated by a single AP, the following parameter values were reported for slow-twitch (soleus) fibers versus fast-twitch (EDL) fibers: (a) time of peak and FDHM of twitch tension: 97 and 480 ms versus 23 and 97 ms, respectively; (b) peak amplitude and FDHM of $\Delta[Ca^{2+}]$: 9 µM and 4.4 ms versus 21 µM and 2.0 ms; and (c) the amount and peak rate of SR Ca^{2+} release: 120 µM and 105 µM/ms versus 358 µM and 473 µM/ms (Baylor and Hollingworth, 2003). These relative differences between fiber types are quite similar to those reported above at 16°C, and it is reasonable to believe that similar relative differences apply under fully physiological conditions.

Summary

The waveforms in Fig. 4 provide detailed estimates of the major myoplasmic Ca^{2+} movements that take place in mouse slow-twitch and fast-twitch fibers during twitches and brief tetani. Although it is too much to expect that all aspects of these comparisons are error free, we believe that the basic features shown in Fig. 4 provide a reasonable working model of Ca^{2+} signaling in the two fiber types. Hopefully, future measurements will permit corrections and refinements of the estimated Ca^{2+} movements. The analysis reveals that, for comparable stimuli, slow-twitch fibers release ~0.3 times the amount of SR Ca^{2+} as fast-twitch fibers. A corollary prediction is that, to resequester the released Ca^{2+}, the SR Ca^{2+} pumps in slow-twitch fibers consume ~0.3 times the ATP as that in fast-twitch fibers. This factor is similar to that which characterizes the total ATP consumption during brief contractions of slow-twitch versus fast-twitch fibers (20°C; Crow and Kushmerick, 1982); in this case, however, the ATP consumption is mainly caused by myosin, with a minor fraction caused by the SR Ca^{2+} pumps (Barclay et al., 2007).

One interesting avenue for future investigation concerns the time course with which $\Delta[Ca^{2+}]$ declines to zero after stimuli like those in Fig. 2. In both slow-twitch and fast-twitch fibers, our measurements with high-affinity fluorescent Ca^{2+} indicators reveal that this decline—and hence the time of pumping Ca^{2+} back into the SR—continues for some seconds (16°C). It remains to be determined how well the model predictions of $\Delta[Ca^{2+}]$ on this slow time scale agree with these measurements. Another avenue concerns the properties of $\Delta[Ca^{2+}]$ and the associated myoplasmic Ca^{2+} movements in fibers of the fast-twitch oxidative subtype (fatigue-resistant fast-twitch fibers; Berchtold et al., 2000; Schiaffino and Reggiani, 2011), which are not considered here. In mice, these fibers make up a significant fraction of the fibers in both soleus and EDL muscles (e.g., Crow and Kushmerick, 1982; Haida et al., 1989; Maréchal et al., 1995; Allen et al., 2001; Asmussen et al., 2003), and they remain to be studied with the methods described in this article.

We thank Drs. E. Michael Ostap and Lawrence C. Rome for comments on an early version of the manuscript.

This work was supported by grants from the U.S. National Institutes of Health (GM 086167) and the Muscular Dystrophy Association.

Richard L. Moss served as editor.

Submitted: 13 January 2012
Accepted: 16 February 2012

REFERENCES

Allen, D.G., G.D. Lamb, and H. Westerblad. 2008. Skeletal muscle fatigue: cellular mechanisms. *Physiol. Rev.* 88:287–332. http://dx.doi.org/10.1152/physrev.00015.2007

Allen, D.L., B.C. Harrison, C. Sartorius, W.C. Byrnes, and L.A. Leinwand. 2001. Mutation of the IIB myosin heavy chain gene results in muscle fiber loss and compensatory hypertrophy. *Am. J. Physiol. Cell Physiol.* 280:C637–C645.

Andrade, F.H., C.A. McMullen, and R.E. Rumbaut. 2005. Mitochondria are fast Ca^{2+} sinks in rat extraocular muscles: a novel regulatory influence on contractile function and metabolism. *Invest. Ophthalmol. Vis. Sci.* 46:4541–4547. http://dx.doi.org/10.1167/iovs.05-0809

Appelt, D., V. Shen, and C. Franzini-Armstrong. 1991. Quantitation of Ca ATPase, feet and mitochondria in superfast muscle fibres from the toadfish, *Opsanus tau*. *J. Muscle Res. Cell Motil.* 12:543–552. http://dx.doi.org/10.1007/BF01738442

Asmussen, G., I. Schmalbruch, T. Soukup, and D. Pette. 2003. Contractile properties, fiber types, and myosin isoforms in fast and slow muscles of hyperactive Japanese waltzing mice. *Exp. Neurol.* 184:758–766. http://dx.doi.org/10.1016/S0014-4886(03)00294-2

Barclay, C.J., R.C. Woledge, and N.A. Curtin. 2007. Energy turnover for Ca^{2+} cycling in skeletal muscle. *J. Muscle Res. Cell Motil.* 28:259–274. http://dx.doi.org/10.1007/s10974-007-9116-7

Baylor, S.M., and S. Hollingworth. 1988. Fura-2 calcium transients in frog skeletal muscle fibres. *J. Physiol.* 403:151–192.

Baylor, S.M., and S. Hollingworth. 1998. Model of sarcomeric Ca^{2+} movements, including ATP Ca^{2+} binding and diffusion, during activation of frog skeletal muscle. *J. Gen. Physiol.* 112:297–316. http://dx.doi.org/10.1085/jgp.112.3.297

Baylor, S.M., and S. Hollingworth. 2003. Sarcoplasmic reticulum calcium release compared in slow-twitch and fast-twitch fibres of mouse muscle. *J. Physiol.* 551:125–138. http://dx.doi.org/10.1113/jphysiol.2003.041608

Baylor, S.M., and S. Hollingworth. 2007. Simulation of Ca^{2+} movements within the sarcomere of fast-twitch mouse fibers stimulated by action potentials. *J. Gen. Physiol.* 130:283–302. http://dx.doi.org/10.1085/jgp.200709827

Baylor, S.M., and S. Hollingworth. 2011. Calcium indicators and calcium signalling in skeletal muscle fibres during excitation-contraction coupling. *Prog. Biophys. Mol. Biol.* 105:162–179. http://dx.doi.org/10.1016/j.pbiomolbio.2010.06.001

Baylor, S.M., W.K. Chandler, and M.W. Marshall. 1983. Sarcoplasmic reticulum calcium release in frog skeletal muscle fibres estimated from Arsenazo III calcium transients. *J. Physiol.* 344:625–666.

Baylor, S.M., S. Hollingworth, and W.K. Chandler. 2002. Comparison of simulated and measured calcium sparks in intact skeletal muscle fibers of the frog. *J. Gen. Physiol.* 120:349–368. http://dx.doi.org/10.1085/jgp.20028620

Berchtold, M.W., H. Brinkmeier, and M. Müntener. 2000. Calcium ion in skeletal muscle: its crucial role for muscle function, plasticity, and disease. *Physiol. Rev.* 80:1215–1265.

Bottinelli, R., M. Canepari, C. Reggiani, and G.J.M. Stienen. 1994. Myofibrillar ATPase activity during isometric contraction and isomyosin composition in rat single skinned muscle fibres. *J. Physiol.* 481:663–675.

Brown, I.E., D.H. Kim, and G.E. Loeb. 1998. The effect of sarcomere length on triad location in intact feline caudofeomoralis muscle fibres. *J. Muscle Res. Cell Motil.* 19:473–477. http://dx.doi.org/10.1023/A:1005309107903

Calderón, J.C., P. Bolaños, S.H. Torres, G. Rodríguez-Arroyo, and C. Caputo. 2009. Different fibre populations distinguished by their calcium transient characteristics in enzymatically dissociated murine *flexor digitorum brevis* and *soleus* muscles. *J. Muscle Res. Cell Motil.* 30:125–137. http://dx.doi.org/10.1007/s10974-009-9181-1

Calderón, J.C., P. Bolaños, and C. Caputo. 2010. Myosin heavy chain isoform composition and Ca^{2+} transients in fibres from enzymatically dissociated murine soleus and extensor digitorum longus muscles. *J. Physiol.* 588:267–279. http://dx.doi.org/10.1113/jphysiol.2009.180893

Cannell, M.B., and D.G. Allen. 1984. Model of calcium movements during activation in the sarcomere of frog skeletal muscle. *Biophys. J.* 45:913–925. http://dx.doi.org/10.1016/S0006-3495(84)84238-1

Capote, J., P. Bolaños, R.P. Schuhmeier, W. Melzer, and C. Caputo. 2005. Calcium transients in developing mouse skeletal muscle fibres. *J. Physiol.* 564:451–464. http://dx.doi.org/10.1113/jphysiol.2004.081034

Carroll, S.L., M.G. Klein, and M.F. Schneider. 1997. Decay of calcium transients after electrical stimulation in rat fast- and slow-twitch skeletal muscle fibres. *J. Physiol.* 501:573–588. http://dx.doi.org/10.1111/j.1469-7793.1997.573bm.x

Claflin, D.R., D.L. Morgan, D.G. Stephenson, and F.J. Julian. 1994. The intracellular Ca^{2+} transient and tension in frog skeletal muscle fibres measured with high temporal resolution. *J. Physiol.* 475:319–325.

Close, R.I. 1967. Properties of motor units in fast and slow skeletal muscles of the rat. *J. Physiol.* 193:45–55.

Crow, M.T., and M.J. Kushmerick. 1982. Chemical energetics of slow- and fast-twitch muscles of the mouse. *J. Gen. Physiol.* 79:147–166. http://dx.doi.org/10.1085/jgp.79.1.147

Danieli-Betto, D., R. Betto, and M. Midrio. 1990. Calcium sensitivity and myofibrillar protein isoforms of rat skinned skeletal muscle fibres. *Pflugers Arch.* 417:303–308. http://dx.doi.org/10.1007/BF00370996

Davis, J.P., C. Norman, T. Kobayashi, R.J. Solaro, D.R. Swartz, and S.B. Tikunova. 2007. Effects of thin and thick filament proteins on calcium binding and exchange with cardiac troponin C. *Biophys. J.* 92:3195–3206. http://dx.doi.org/10.1529/biophysj.106.095406

Decrouy, A., P.C. Even, and A. Chinet. 1993. Decreased rates of Ca^{2+}-dependent heat production in slow- and fast-twitch muscles from the dystrophic (*mdx*) mouse. *Experientia.* 49:843–849. http://dx.doi.org/10.1007/BF01952595

Delbono, O., and G. Meissner. 1996. Sarcoplasmic reticulum Ca^{2+} release in rat slow- and fast-twitch muscles. *J. Membr. Biol.* 151:123–130. http://dx.doi.org/10.1007/s002329900063

Delbono, O., and E. Stefani. 1993. Calcium transients in single mammalian skeletal muscle fibres. *J. Physiol.* 463:689–707.

Eisenberg, B.R. 1983. Quantitative ultrastructure of mammalian skeletal muscle. *In* Handbook of Physiology Section 10: Skeletal Muscle. L.D. Peachey, R.H. Adrian, and S.R. Geiger, editors. Williams and Wilkins, Baltimore, MD. 73–112.

Escobar, A.L., J.R. Monck, J.M. Fernandez, and J.L. Vergara. 1994. Localization of the site of Ca^{2+} release at the level of a single sarcomere in skeletal muscle fibres. *Nature.* 367:739–741. http://dx.doi.org/10.1038/367739a0

Ferguson, D.G., and C. Franzini-Armstrong. 1988. The Ca^{2+} ATPase content of slow and fast twitch fibers of guinea pig. *Muscle Nerve.* 11:561–570. http://dx.doi.org/10.1002/mus.880110607

Franzini-Armstrong, C., and G. Nunzi. 1983. Junctional feet and particles in the triads of a fast-twitch muscle fibre. *J. Muscle Res. Cell Motil.* 4:233–252. http://dx.doi.org/10.1007/BF00712033

Franzini-Armstrong, C., D.G. Ferguson, and C. Champ. 1988. Discrimination between fast- and slow-twitch fibres of guinea pig skeletal muscle using the relative surface density of junctional transverse tubule membrane. *J. Muscle Res. Cell Motil.* 9:403–414. http://dx.doi.org/10.1007/BF01774067

Fuchs, F., and M. Bayuk. 1976. Cooperative binding of calcium to glycerinated skeletal muscle fibers. *Biochim. Biophys. Acta.* 440:448–455. http://dx.doi.org/10.1016/0005-2728(76)90077-3

Gillis, J.M., D. Thomason, J. Lefèvre, and R.H. Kretsinger. 1982. Parvalbumins and muscle relaxation: a computer simulation study. *J. Muscle Res. Cell Motil.* 3:377–398. http://dx.doi.org/10.1007/BF00712090

Gómez, J., P. Neco, M. DiFranco, and J.L. Vergara. 2006. Calcium release domains in mammalian skeletal muscle studied with two-photon imaging and spot detection techniques. *J. Gen. Physiol.* 127:623–637. http://dx.doi.org/10.1085/jgp.200509475

González, E., M.L. Messi, and O. Delbono. 2000. The specific force of single intact *extensor digitorum longus* and *soleus* mouse muscle fibers declines with aging. *J. Membr. Biol.* 178:175–183. http://dx.doi.org/10.1007/s002320010025

Grabarek, Z., J. Grabarek, P.C. Leavis, and J. Gergely. 1983. Cooperative binding to the Ca^{2+}-specific sites of troponin C in regulated actin and actomyosin. *J. Biol. Chem.* 258:14098–14102.

Grynkiewicz, G., M. Poenie, and R.Y. Tsien. 1985. A new generation of Ca^{2+} indicators with greatly improved fluorescence properties. *J. Biol. Chem.* 260:3440–3450.

Haida, N., W.M. Fowler Jr., R.T. Abresch, D.B. Larson, R.B. Sharman, R.G. Taylor, and R.K. Entrikin. 1989. Effect of hind-limb suspension on young and adult skeletal muscle. I. Normal mice. *Exp. Neurol.* 103:68–76. http://dx.doi.org/10.1016/0014-4886(89)90187-8

Hamoir, G., N. Gerardin-Otthiers, and B. Focant. 1980. Protein differentiation of the superfast swimbladder muscle of the toadfish *Opsanus tau*. *J. Mol. Biol.* 143:155–160. http://dx.doi.org/10.1016/0022-2836(80)90129-1

Harwood, C.L., I.S. Young, B.A. Tikunov, S. Hollingworth, S.M. Baylor, and L.C. Rome. 2011. Paying the piper: the cost of Ca^{2+} pumping during the mating call of toadfish. *J. Physiol.* 589:5467–5484. http://dx.doi.org/10.1113/jphysiol.2011.211979

Heizmann, C.W., M.W. Berchtold, and A.M. Rowlerson. 1982. Correlation of parvalbumin concentration with relaxation speed in mammalian muscles. *Proc. Natl. Acad. Sci. USA.* 79:7243–7247. http://dx.doi.org/10.1073/pnas.79.23.7243

Hess, A. 1970. Vertebrate slow muscle fibers. *Physiol. Rev.* 50:40–62.

Hirota, A., W.K. Chandler, P.L. Southwick, and A.S. Waggoner. 1989. Calcium signals recorded from two new purpurate indicators inside frog cut twitch fibers. *J. Gen. Physiol.* 94:597–631. http://dx.doi.org/10.1085/jgp.94.4.597

Hoh, J.F.Y. 2002. 'Superfast' or masticatory myosin and the evolution of jaw-closing muscles of vertebrates. *J. Exp. Biol.* 205:2203–2210.

Hollingworth, S., and M.W. Marshall. 1981. A comparative study of charge movement in rat and frog skeletal muscle fibres. *J. Physiol.* 321:583–602.

Hollingworth, S., M. Zhao, and S.M. Baylor. 1996. The amplitude and time course of the myoplasmic free $[Ca^{2+}]$ transient in fast-twitch fibers of mouse muscle. *J. Gen. Physiol.* 108:455–469. http://dx.doi.org/10.1085/jgp.108.5.455

Hollingworth, S., C. Soeller, S.M. Baylor, and M.B. Cannell. 2000. Sarcomeric Ca^{2+} gradients during activation of frog skeletal muscle fibres imaged with confocal and two-photon microscopy. *J. Physiol.* 526:551–560. http://dx.doi.org/10.1111/j.1469-7793.2000.t01-1-00551.x

Hollingworth, S., W.K. Chandler, and S.M. Baylor. 2006. Effects of tetracaine on voltage-activated calcium sparks in frog intact skeletal muscle fibers. *J. Gen. Physiol.* 127:291–307. http://dx.doi.org/10.1085/jgp.200509477

Hollingworth, S., U. Zeiger, and S.M. Baylor. 2008. Comparison of the myoplasmic calcium transient elicited by an action potential in intact fibres of *mdx* and normal mice. *J. Physiol.* 586:5063–5075. http://dx.doi.org/10.1113/jphysiol.2008.160507

Hollingworth, S., K.R. Gee, and S.M. Baylor. 2009. Low-affinity Ca^{2+} indicators compared in measurements of skeletal muscle Ca^{2+} transients. *Biophys. J.* 97:1864–1872. http://dx.doi.org/10.1016/j.bpj.2009.07.021

Hollingworth, S., M.M. Kim, and S.M. Baylor. 2012. Measurement and simulation of myoplasmic calcium transients in mouse slow-twitch muscle fibres. *J. Physiol.* 590:575–594. http://dx.doi.org/10.1113/jphysiol.2011.220780

Inesi, G., T. Watanabe, C. Coan, and A. Murphy. 1982. The mechanism of sarcoplasmic reticulum ATPase. *Ann. NY Acad. Sci.* 402:515–534. http://dx.doi.org/10.1111/j.1749-6632.1982.tb25772.x

Jackman, M.R., and W.T. Willis. 1996. Characteristics of mitochondria isolated from type I and type IIb skeletal muscle. *Am. J. Physiol.* 270:C673–C678.

Jiang, Y.-H., M.G. Klein, and M.F. Schneider. 1999. Numerical simulation of Ca^{2+} "sparks" in skeletal muscle. *Biophys. J.* 77:2333–2357. http://dx.doi.org/10.1016/S0006-3495(99)77072-4

Jong, D.-S., P.C. Pape, S.M. Baylor, and W.K. Chandler. 1995. Calcium inactivation of calcium release in frog cut muscle fibers that contain millimolar EGTA or Fura-2. *J. Gen. Physiol.* 106:337–388. http://dx.doi.org/10.1085/jgp.106.2.337

Kerrick, W.G.L., D. Secrist, R. Coby, and S. Lucas. 1976. Development of difference between red and white muscles in sensitivity to Ca^{2+} in the rabbit from embryo to adult. *Nature.* 260:440–441. http://dx.doi.org/10.1038/260440a0

Konishi, M., S. Hollingworth, A.B. Harkins, and S.M. Baylor. 1991. Myoplasmic calcium transients in intact frog skeletal muscle fibers monitored with the fluorescent indicator furaptra. *J. Gen. Physiol.* 97:271–301. http://dx.doi.org/10.1085/jgp.97.2.271

Kushmerick, M.J., T.S. Moerland, and R.W. Wiseman. 1992. Mammalian skeletal muscle fibers distinguished by contents of phosphocreatine, ATP, and P_i. *Proc. Natl. Acad. Sci. USA.* 89:7521–7525. http://dx.doi.org/10.1073/pnas.89.16.7521

Lamb, G.D., and T.D. Walsh. 1987. Calcium currents, charge movement and dihydropyridine binding in fast- and slow-twitch muscles of rat and rabbit. *J. Physiol.* 393:595–617.

Leberer, E., and D. Pette. 1986. Immunochemical quantification of sarcoplasmic reticulum Ca-ATPase, of calsequestrin and of parvalbumin in rabbit skeletal muscles of defined fiber composition. *Eur. J. Biochem.* 156:489–496. http://dx.doi.org/10.1111/j.1432-1033.1986.tb09607.x

Lytton, J., M. Westlin, S.E. Burk, G.E. Shull, and D.H. MacLennan. 1992. Functional comparisons between isoforms of the sarcoplasmic or endoplasmic reticulum family of calcium pumps. *J. Biol. Chem.* 267:14483–14489.

Maréchal, G., G.R. Coulton, and G. Beckers-Bleukx. 1995. Mechanical power and myosin composition of soleus and extensor digitorum longus muscles of *ky* mice. *Am. J. Physiol.* 268:C513–C519.

Melzer, W., E. Rios, and M.F. Schneider. 1987. A general procedure for determining the rate of calcium release from the sarcoplasmic reticulum in skeletal muscle fibers. *Biophys. J.* 51:849–863. http://dx.doi.org/10.1016/S0006-3495(87)83413-6

Metzger, J.M., and R.L. Moss. 1990. Calcium-sensitive cross-bridge transitions in mammalian fast and slow skeletal muscle fibers. *Science.* 247:1088–1090. http://dx.doi.org/10.1126/science.2309121

Naraghi, M. 1997. T-jump study of calcium binding kinetics of calcium chelators. *Cell Calcium.* 22:255–268. http://dx.doi.org/10.1016/S0143-4160(97)90064-6

Norris, S.M., E. Bombardier, I.C. Smith, C. Vigna, and A.R. Tupling. 2010. ATP consumption by sarcoplasmic reticulum Ca^{2+} pumps accounts for 50% of resting metabolic rate in mouse fast and slow twitch skeletal muscle. *Am. J. Physiol. Cell Physiol.* 298:C521–C529. http://dx.doi.org/10.1152/ajpcell.00479.2009

Novo, D., M. DiFranco, and J.L. Vergara. 2003. Comparison between the predictions of diffusion-reaction models and localized Ca^{2+} transients in amphibian skeletal muscle fibers. *Biophys. J.* 85:1080–1097. http://dx.doi.org/10.1016/S0006-3495(03)74546-9

Potter, J.D., J.D. Johnson, J.R. Dedman, W.E. Schreiber, F. Mandel, R.L. Jackson, and A.R. Means. 1977. Calcium-binding proteins: relationship of binding, structure, conformation and biological function. *In* Calcium-Binding Proteins and Calcium Function. R.H. Wasserman, R.A. Corradino, E. Carofoli, R.H. Kretsinger, D.H. MacLennan, and F.L. Siegel, editors. Elsevier, Amsterdam. 239–250.

Racay, P., P. Gregory, and B. Schwaller. 2006. Parvalbumin deficiency in fast-twitch muscles leads to increased 'slow-twitch type' mitochondria, but does not affect the expression of fiber specific proteins. *FEBS J.* 273:96–108. http://dx.doi.org/10.1111/j.1742-4658.2005.05046.x

Raju, B., E. Murphy, L.A. Levy, R.D. Hall, and R.E. London. 1989. A fluorescent indicator for measuring cytosolic free magnesium. *Am. J. Physiol.* 256:C540–C548.

Ríos, E., and G. Brum. 1987. Involvement of dihydropyridine receptors in excitation-contraction coupling in skeletal muscle. *Nature.* 325:717–720. http://dx.doi.org/10.1038/325717a0

Robertson, S.P., J.D. Johnson, and J.D. Potter. 1981. The time-course of Ca^{2+} exchange with calmodulin, troponin, parvalbumin, and myosin in response to transient increases in Ca^{2+}. *Biophys. J.* 34:559–569. http://dx.doi.org/10.1016/S0006-3495(81)84868-0

Rolfe, D.F.S., and G.C. Brown. 1997. Cellular energy utilization and molecular origin of standard metabolic rate in mammals. *Physiol. Rev.* 77:731–758.

Rome, L.C., D.A. Syme, S. Hollingworth, S.L. Lindstedt, and S.M. Baylor. 1996. The whistle and the rattle: the design of sound producing muscles. *Proc. Natl. Acad. Sci. USA.* 93:8095–8100. http://dx.doi.org/10.1073/pnas.93.15.8095

Ruff, R.L. 1989. Calcium sensitivity of fast- and slow-twitch human muscle fibers. *Muscle Nerve.* 12:32–37. http://dx.doi.org/10.1002/mus.880120107

Schiaffino, S., and C. Reggiani. 2011. Fiber types in mammalian skeletal muscles. *Physiol. Rev.* 91:1447–1531. http://dx.doi.org/10.1152/physrev.00031.2010

Schneider, M.F., and W.K. Chandler. 1973. Voltage dependent charge movement of skeletal muscle: a possible step in excitation-contraction coupling. *Nature.* 242:244–246. http://dx.doi.org/10.1038/242244a0

Schneider, M.F., and B.J. Simon. 1988. Inactivation of calcium release from the sarcoplasmic reticulum in frog skeletal muscle. *J. Physiol.* 405:727–745.

Schwerzmann, K., H. Hoppeler, S.R. Kayar, and E.R. Weibel. 1989. Oxidative capacity of muscle and mitochondria: correlation of physiological, biochemical, and morphometric characteristics. *Proc. Natl. Acad. Sci. USA.* 86:1583–1587. http://dx.doi.org/10.1073/pnas.86.5.1583

Smith, D.S. 1966. The organization and function of the sarcoplasmic reticulum and T-system of muscle cells. *Prog. Biophys. Mol. Biol.* 16:107–142. http://dx.doi.org/10.1016/0079-6107(66)90004-6

Stephenson, D.G., and D.A. Williams. 1981. Calcium-activated force responses in fast- and slow-twitch skinned muscle fibres of the rat at different temperatures. *J. Physiol.* 317:281–302.

Sweeney, H.L., R.M.M. Brito, P.R. Rosevear, and J.A. Putkey. 1990. The low-affinity Ca^{2+}-binding sites in cardiac/slow skeletal muscle troponin C perform distinct functions: site I alone cannot trigger contraction. *Proc. Natl. Acad. Sci. USA.* 87:9538–9542. http://dx.doi.org/10.1073/pnas.87.24.9538

Tanabe, T., K.G. Beam, J.A. Powell, and S. Numa. 1988. Restoration of excitation-contraction coupling and slow calcium current in dysgenic muscle by dihydropyridine receptor complementary DNA. *Nature.* 336:134–139. http://dx.doi.org/10.1038/336134a0

Tikunov, B.A., and L.C. Rome. 2009. Is high concentration of parvalbumin a requirement for superfast relaxation? *J. Muscle Res. Cell Motil.* 30:57–65. http://dx.doi.org/10.1007/s10974-009-9175-z

Unsworth, B.R., F.A. Witzmann, and R.H. Fitts. 1982. A comparison of rat myosin from fast and slow skeletal muscle and the effect of disuse. *J. Biol. Chem.* 257:15129–15136.

van Eerd, J.P., and K. Takahashi. 1976. Determination of the complete amino acid sequence of bovine cardiac troponin C. *Biochemistry.* 15:1171–1180. http://dx.doi.org/10.1021/bi00650a033

Weber, A., R. Herz, and I. Reiss. 1966. Study of the kinetics of calcium transport by isolated fragmented sarcoplasmic reticulum. *Biochem. Z.* 345:329–369.

Wu, K.-D., and J. Lytton. 1993. Molecular cloning and quantification of sarcoplasmic reticulum Ca^{2+}-ATPase isoforms in rat muscles. *Am. J. Physiol.* 264:C333–C341.

Yamaguchi, N., B.L. Prosser, F. Ghassemi, L. Xu, D.A. Pasek, J.P. Eu, E.O. Hernández-Ochoa, B.R. Cannon, P.T. Wilder, R.M. Lovering, et al. 2011. Modulation of sarcoplasmic reticulum Ca^{2+} release in skeletal muscle expressing ryanodine receptor impaired in regulation by calmodulin and S100A1. *Am. J. Physiol. Cell Physiol.* 300:C998–C1012. http://dx.doi.org/10.1152/ajpcell.00370.2010

Young, I.S., C.L. Harwood, and L.C. Rome. 2003. Cross-bridge blocker BTS permits direct measurement of SR Ca^{2+} pump ATP utilization in toadfish swimbladder muscle fibers. *Am. J. Physiol. Cell Physiol.* 285:C781–C787.